Green Chemistry

Accepted Manuscript

ROYAL SOCIETY OF CHEMISTRY

www.rsc.org/greenchem

Understanding Pretreatment Efficacy of Four Cholinium and Imidazolium Ionic Liquids by Chemistry and Computation

Ning Sun[a,b], Ramakrishnan Parthasarathi[a,c], Aaron M. Socha[a,c,d], Jian Shi[a,c], Sonny Zhang[a], Vitalie Stavila[c], Kenneth L. Sale[a,c], Blake A. Simmons[a,c] and Seema Singh[a,c]*

[a]Deconstruction Division, Joint BioEnergy Institute, Emeryville, CA

[b]Physical Biosciences Division, Lawrence Berkeley National Laboratory, Berkeley, CA, USA

[c]Biological and Materials Sciences Center, Sandia National Laboratories, Livermore, CA, USA

[d]Department of Chemistry and Chemical Technology, Bronx Community College, Bronx, NY, USA

Abstract

Certain ionic liquids (ILs) offer a potentially more sustainable and environmentally responsible alternative to organic solvents for many industrial applications, including biorefineries, where they are used to pretreat lignocellulose. To develop a more robust understanding on the roles of cations and anions on the process, we monitored the impact of the respective ILs on *Panicum virgatum* (switchgrass) in terms of lignin content, cellulose crystallinity, and enzymatic digestibility. The behaviors of four ILs, based on one of two cations, 1-ethyl-3-methylimidazolium ($[C_2mim]^+$) and cholinium ($[Ch]^+$), and one of two anions, acetate ($[OAc]^-$) and lysinate ($[Lys]^-$), were compared. While all four ILs were effective in pretreating switchgrass, ILs containing $[Lys]^-$ anions provided greater delignification (70-80% vs. 16-50%) after addition of water as the anti-solvent and higher glucose yields (78-96% vs. 56-90%) compared to those obtained by use of ILs containing $[OAc]^-$ anions. Measurements of the Kamlet-Taft parameters using a series of dyes indicated a greater hydrogen bond basicity for the ILs with $[Lys]^-$ anion as compared to acetate ILs. To understand the effective delignification ability of lysinate-based ILs, interaction energies of individual ions and ion pairs with a model dilignol substrate were determined by quantum chemical calculations. The results show that the addition of antisolvent significantly influenced the interaction energies governing lignin removal during the process.

Keywords: Ionic Liquid Pretreatment, Biomass Pretreatment, Biofuels, Delignification, Kamlet-Taft Parameters, Quantum Chemistry

1. Background

Following an initial report of cellulose dissolution in certain ionic liquids (ILs),[1] significant research efforts have been devoted to biomass processing using these remarkable solvents. Certain imidazolium-based ILs are known to efficiently solvate many types of biomass, and allow facile recovery of cellulose upon addition of an anti-solvent such as water or alcohols.[2-10] The highest cellulose solubilities are obtained using 1-ethyl-3-methylimidazolium acetate ([C_2mim][OAc]), which has a minimal impact on the environment and low toxicity to animals and humans.[11]

It has been shown that anions play a critical role in cellulose solubilization, and those that accept hydrogen bonds from cellulose hydroxyl protons can effectively disrupt the inter- and intra-molecular hydrogen bonding in cellulose.[12] This phenomenon is governed by hydrogen bond basicity (β), one of the three solvent parameters quantified using the Kamlet-Taft (K-T) system, which also define a solvent's polarity parameters in terms of hydrogen bond acidity (α) and polarizability (π*).[13] Since the β value quantifies an IL's ability to accept a hydrogen bond, its magnitude is primarily determined by the anion.[14] ILs with higher β values,[15] and more recently reported, ILs with larger differences between β and α, i.e. net basicity (β-α),[16] tend to dissolve cellulose more efficiently. Upon precipitation with anti-solvent (such as water or alcohols), the regenerated cellulose often has reduced crystallinity and is easily enzymatically digested by cellulase. Hydrogen bond basicity not only affects an IL's capacity to dissolve and/or swell lignocellulose,[17] but also acts as a predictor of biomass pretreatment efficacy.[18] ILs with higher β values significantly remove lignin, reduce cellulose crystallinity, and result in higher glucose yields after enzymatic saccharification.[18]

Recently, ILs containing cholinium cations and amino acid anions ([Ch][AA]), referred to as "bionic liquids",[19] were shown to efficiently pretreat rice straw by selectively removing lignin. The ILs are prepared from naturally occurring, renewable starting materials and are thus expected to be more biocompatible to enzymes and microbes than acetate-based ILs, and potentially less costly compared to imidazolium-based ILs. After pretreatment of rice straw at

90 ºC for 5 h, sugar yields (percentage of glucose or xylose in untreated rice straw) of 84% glucose and 42.1% xylose were achieved for [Ch][Lys]. Since cellulose is sparingly soluble in [Ch][AA], the pretreated rice straw showed increased crystallinity due to removal of amorphous hemicelluloses and lignin.[19] The efficiency of IL pretreatment of biomass is thought to result from: 1) dissolution of cellulose and subsequent reduction of its crystallinity coupled with delignification;[7, 9] 2) selective delignification without cellulose dissolution.[10, 19, 20]

Most of the work to date on IL pretreatment has been empirical in nature, and there is no well-accepted understanding of the detailed mechanism of pretreatment. In the work presented here, the chemistry of IL pretreatment is examined by use of four ILs, composed of two cations, 1-ethyl-3-methylimidazolium ($[C_2mim]^+$) and cholinium ($[Ch]^+$), in combination with two anions, acetate ($[OAc]^-$) and lysinate ($[Lys]^-$) (Figure 1) to pretreat biomass and then determine sugar release by enzymatic saccharification of the pretreated biomass (after removal of the residual IL by washing with DI water) using identical feedstock, pretreatment conditions, and enzyme cocktail for saccharification. The interactions of individual ions and ion pairs with a lignin model compound were determined to examine the mechanistic nature of dissolution of lignin in ILs and provide a rationale for the effects of various cations and anions. This combined approach provides additional insights into the roles of specific cations and anions in biomass pretreatment applications.

2. Experimental

2.1 Raw materials

Switchgrass (*Panicum virgatum*) was kindly provided from the laboratory of Prof. Daniel Putnam at the University of California, Davis. The switchgrass studied was a combination of lowland and upland varieties, grown in Davis, California and harvested in 2011. The samples were ground using a Thomas-Wiley® Mill fitted with a 20-mesh screen (Model 3383-L10 Arthur H. Thomas Co., Philadelphia, PA, USA) and used without further sieving. The samples were stored at 4 °C in a sealed plastic bag for use in all experiments. Commercial enzyme

cocktails Cellic® CTec 2 and HTec 2 were generously provided by Novozymes (Davis, CA). The ILs [C_2mim][OAc] (>95% purity) and cholinium acetate ([Ch][OAc]) were purchased from BASF (Ludwigshafen, Germany). Choline hydroxide (46% in H_2O), L-lysine (>98%), Barium hydroxide ($Ba(OH)_2$), 4-Nitroaninline (4NA), N,N-diethyl-4-nitroaniline (DENA), and Reichardt's dye (RD) were purchased from Sigma-Aldrich (St. Louis, MO) and used without further purification. 1-ethyl-3-methylimidazolium hydrogen sulfate ([C_2mim][HSO_4]) (>98% purity) was purchased from IoLiTec Inc. (Heilbronn, Germany). Organosolv lignin was provided by Lignol Energy Corporation (Burnaby, BC, Canada).

2.2 Synthesis of [C_2mim][Lys] and [Ch][Lys]

[Ch][Lys] and [C_2mim][Lys] were synthesized according to literature precedents,[21, 22] and a detailed procedure can be found in the supplementary information. In summary, [Ch][Lys] was prepared by adding 1 equivalent of aqueous [Ch][OH] to 1.2 equivalents of aqueous L-lysine at 4 °C. After stirring for 48 h in the dark, water was removed under reduced pressure at 50-55°C. Excess lysine was removed by precipitation using a solution of acetonitrile/methanol (9:1, v/v), stirring vigorously and centrifuging. The supernatant was concentrated with a rotary evaporator and then dried in vacuum oven at 70 °C for 48 h to provide the desired product. [C_2mim][Lys] was synthesized in two steps. The unstable [C_2mim][OH] intermediate was prepared *in situ* by reacting [C_2mim][HSO_4] with $Ba(OH)_2$ at 4 °C to give a $BaSO_4$ precipitate which was removed by centrifugation. The supernatant, an aqueous solution of [C_2mim][OH], was reacted with 1.2 equivalents of an aqueous solution of L-lysine to provide the desired product. The structures of the ILs were confirmed by comparison of their ^{1}H NMR spectra to published data (See ESI, Figure S1-S2).[21, 22]

2.3 Biomass pretreatment

A 10% (w/w) biomass solution was carefully prepared by combining 2 g of switchgrass with 18 g of IL in a 50 mL globe reactor (Syrris). The reactor was heated to the desired temperature and stirred at 300 rpm with a Teflon overhead stirrer. All pretreatment reactions were conducted in duplicate. Following pretreatment, 100 mL of deionized (DI) water was slowly added to the biomass/IL slurry with continued stirring. The mixture was transferred to 50 mL

Falcon tubes and centrifuged at high speed (14,000 rpm) to separate solids. Additional solids were collected from the supernatant using nylon mesh filtration (1 micron pore size), and the combined pretreated biomass was washed with an additional 100 mL of DI water to remove any residual IL. The solids were again filtered through 1 micron nylon mesh and stored at 4ºC for analysis.

2.4 Lignin solubility test

Organosolv lignin was used as a model compound for lignin solubility tests in all four ILs studied. A series of different lignin concentrations in the four ILs were prepared and the mixture was agitated in a thermomixer (22331 Hamburg) at 25 and 90 ºC for 2 h. The dissolution was checked under an optical microscope at 40 x.

2.5 Analysis and characterization methods

Moisture content of pretreated switchgrass was quantified using a moisture content analyzer (Mettler Toledo, Model HB43-S Halogen) by heating to 105 ºC and monitoring the mass until it remained constant. The dried biomass was used for compositional analysis.

Compositional analysis Compositional analysis of switchgrass before and after pretreatment was performed using NREL acidolysis protocols (LAP) LAP-002 and LAP-005.[23] Briefly, 200 mg of biomass and 2 mL 72% H_2SO_4 were incubated at 30 °C while shaking at 300 rpm for 1 h. The solution was diluted to 4% H_2SO_4 with 56 mL of DI water and autoclaved for 1 h at 121 °C. The reaction was quenched by placing samples into an ice bath before removing the biomass by filtration. Carbohydrate concentrations were determined from the filtrate by Agilent HPLC 1200 Series equipped with a Bio-Rad Aminex HPX-87H column and a Refractive Index detector. An aqueous solution of H_2SO_4 (4 mM) was used as the mobile phase (0.6 mL/min, column temperature 60 ºC). The injection volume was 20 µL with a run time of 25 min. Acid insoluble lignin was quantified gravimetrically from the solid after heating overnight at 105 °C (the weight of acid-insoluble lignin + ash) and then 575 °C for at least 6 h (the weight of ash).

Enzymatic saccharification Enzymatic saccharification of pretreated and untreated biomass was carried out using commercially available enzymes, Cellic® CTec2 and HTec2 from Novozymes, at 50 °C, pH 5.5, and rotation speed of 150 rpm in a rotary incubator

(Enviro-Genie, Scientific Industries, Inc.). All reactions were conducted at 10% biomass loading by placing 500 mg of biomass (dry weight) in a 25 mL centrifuge tube. The pH of the mixture was adjusted to 5.5 with 50 mM sodium citrate buffer (pH 4.8) supplemented with 0.02% NaN_3 to prevent microbial contamination. The total reaction volume (5 mL) included a total protein content of 20 mg protein/g glucan or 5 mg protein/g glucan as determined by compositional analysis. The ratio of CTec2:HTec2 mixtures was held constant at 9:1 for all reactions. Reactions were monitored by centrifuging 50 µL aliquots of supernatant (5 min, 14,000 rpm) at specific time intervals and measuring monomeric sugar concentrations by HPLC as described previously.

Crystal structure analysis The pretreated biomass was dried and characterized with powder X-ray diffraction (PXRD). The data were collected with a PANalytical Empyrean X-ray diffractometer equipped with a PIXcel^{3D} detector and operated at 45 kV and 40 kA using Cu *Kα* radiation (λ= 1.5418 Å). The patterns were collected in the 2θ range of 5 to 55° with a step size of 0.026°, and an exposure time of 300 seconds. A reflection-transmission spinner was used as a sample holder and the spinning rate was set at 8 rpm throughout the experiment. The crystallinity index (CrI) was determined from the crystalline and amorphous peak areas by a curve fitting procedure of the measured diffraction patterns using the software package HighScore Plus® according to Eq. 1:

$$CrI\ \% = \frac{\sum A_{cr.}}{\sum A_{cr.} + \sum A_{am.}} \times 100\% \qquad (1)$$

Kamlet-Taft (K-T) parameters measurement K-T parameters were determined according to previous reports.[18] The three dyes: 4NA, DENA, and RD solutions were prepared in ethanol to a concentration of 1 mg/mL. 2 µL of 4NA, 2 µL of DENA and 20 µL of RD were pipetted into three separate vials and the ethanol was evaporated under a stream of dry nitrogen. Dye concentrations of 12 mM, 8 mM, and 28 mM respectively, were obtained by adding 1.25 mL of the appropriate ILs to each vial and mixing on a shaker at 300 RPM under RT for 30 min. The absorbance spectra at 30, 50, 70, 90, and 110 ºC of each IL/dye solution was measured from 350 to 700 nm using a UV-Vis dual beam spectrophotometer equipped with temperature controller (TMSPC-8, Shimadzu Corporation). K–T parameters for higher temperatures were

estimated by extrapolation of the linear fit of the parameter values obtained experimentally between 30 and 110 ºC.

2.6 Computational methods

The geometries of the two cations, $[C_2mim]^+$ and $[Ch]^+$, and the two anions, $[OAc]^-$ and $[Lys]^-$, and of the lignin dimer model compound of two are rings connected by a β-O-4 linker (Figure 1) were optimized using density functional theory (DFT) with the M06-2X hybrid exchange-correlation functional and the 6-311++G(d, p) basis set. Frequency calculations were carried out to verify that the computed structures corresponded to energy minima. Various initial geometries of the four ILs, $[C_2mim][OAc]$, $[C_2mim][Lys]$, [Ch][OAc], and [Ch][Lys], were modeled with individual cations and anions optimized as described above. A conformational optimization for the dilignol model compound was performed by relaxed potential energy scanning through the dihedral angles of the β-O-4 linkage connecting the two arene rings at the lower level M06-2X/3-21G (d, p), and the resulting minimum energy geometry was reoptimized at the higher level M06-2X/6-311++G(d, p) basis set. Many of the complexes (10-20) of anions and cations interacting with dilignol were constructed based on the prior chemical knowledge of placing ions to the donor and acceptor atoms (see Figure S4 for the electrostatic potentials map) of a dilignol and optimized at M06-2X/3-21G (d, p) basis set. Five low-energy conformations from each ion/ion pair-dilignol complex were further optimized at the higher-level M06-2X/6-31+G (d, p) basis set. The most stable complexes of IL cation and anion with dilignol were used to calculate interaction energies (IEs) at the M06-2X/6-311++G(d, p) level using the supermolecule approach,[24]

$$IE = -\left(E_{Complex} - \sum_{i=1}^{n} E_i \right) \quad (2)$$

where E_{Complex} refer to the energies of cation and anion pair (for IL), anion or cation with dilignol (ion + dilignol), anion and cation with dilignol (ion pair + dilignol) complexes, respectively and E_i refer to the energies of the monomers. The results were corrected for basis set superposition error (BSSE) following the procedure adopted by Boys and Bernardi.[24] All quantum chemical calculations were performed using the Gaussian 09 suite of programs.[25]

3. Results and discussions

3.1 Solid recovery and composition changes

Pretreatment conditions for [Ch][Lys] were optimized at 90 ºC for 5 h since this severity allowed maximum sugar recovery with minimum energy requirement in terms of heating temperature and time.[19] Reports using [C_2mim][OAc] to pretreat biomass have typically used temperatures between 120-160 ºC and time intervals of 1-3 h to achieve high sugar yields.[26] In the present study we chose two pretreatment conditions to get a fair comparison of the four ILs: 90 ºC for 5 h and 140 ºC for 1 h. The effective glass transition temperature (T_g) of lignin was reported to be ~150 ºC and pretreatment of lignocellulosic biomass above this temperature has typically resulted in fast biomass solubilization and high delignification efficiency.[27] By choosing pretreatment temperatures significantly lower than, and close to, the T_g of lignin we wished to determine whether this temperature is crucial for IL pretreatment efficiency and/or it is possible to efficiently pretreat biomass at temperature below 100 ºC. In this paper, we refer to higher temperature pretreatment as the conditions of 140 ºC and 1 h and lower temperature pretreatment as the conditions of 90 ºC and 5 h. [Some IL decomposition is expected under higher temperature pretreatment condition, lower temperature is recommended especially for choline or amino acid based ILs]

Table 1 shows compositional analysis before and after pretreatment with the four ILs studied. Solid recovery refers to the mass percentage of biomass (dry weight) recovered from the original biomass load. After washing, between 51-92% of the biomass was recovered. Generally, pretreatment under higher temperature condition resulted in less solid recovery (90 ºC /5 h = 58-92% vs. 140 ºC /1 h = 51-71%). Three of the major plant cell wall components of switchgrass, glucan, xylan, and acid insoluble lignin, were monitored before and after pretreatment. Untreated switchgrass contained 37.5% glucan, 21.9% xylan and 18.9% acid insoluble lignin. After pretreatment by the four ILs, the glucan loading generally increased and higher temperature resulted in higher glucan contents in pretreated biomass. The exception was found in [C_2mim][Lys] pretreated biomass, whereby the glucan contents were similar

under both conditions (65% vs. 63%). Xylan contents for pretreated biomass were similar to those of the original biomass, occurring within a range of 17-24%. Lignin content of pretreated material generally decreased as compared to the original biomass. This trend was most apparent after pretreatment with [C_2mim][Lys] and [Ch][Lys] where lignin content was reduced by 74% (Untreated: 18.9% vs. pretreated: 5%). The removal or recovery of major components (X) was calculated based on:

$$X\ Recovery\ \% = \frac{W_{pre} \times C_{pre,x}}{W_{SG} \times C_{SG,x}} \times 100\% \qquad (3)$$

$$X\ Removal\ \% = 1 - \frac{W_{pre} \times C_{pre,x}}{W_{SG} \times C_{SG,x}} \times 100\% \qquad (4)$$

where W_{pre} is the mass of pretreated switchgrass, W_{SG} is the mass of untreated switchgrass, $C_{pre,x}$ is the composition of X (glucan, xylan or lignin) in pretreated switchgrass and $C_{SG,x}$ is the composition of X in untreated switchgrass. Because of the different solid recovery, the compositional changes do not always reflect the actual component recovery. For [C_2mim][Lys] and [Ch][OAc], more glucan was removed with increased temperature and decreased pretreatment time, while glucan removal by the other ILs was not observed to be dependent on temperature. Xylan removal was more sensitive to temperature as significantly more xylan was removed at the higher temperature pretreatment, especially for [C_2mim][OAc] (90 ºC /5 h: 1% vs. 140 ºC/1 h: 32%) and [Ch][OAc] (90 ºC/5 h: 2% vs. 140 ºC/1 h: 37%). Higher temperature IL pretreatment facilitated lignin removal (lignin removal at 90 ºC: 17-80% vs. at 140 ºC: 49-87%). These results are consistent with a previous report, where it was found that [Ch][Lys] can extract 60.4% lignin from rice straw after pretreatment at 90 ºC for 24 h. With increased temperatures (130 ºC), up to 71.4% lignin was extracted by [Ch][Lys].[19] Using only DI water as a washing solvent, we observed higher delignification as compared to washing with 0.1 mol/L NaOH, as previously reported.[19] Impressively, pretreatment in [C_2mim][Lys] at 90 ºC and 140 ºC resulted in 80% and 87% lignin removal, respectively. To our knowledge, this is the highest delignification ever reported using ILs as pretreatment solvents.

Lignin solubility of the four ILs was determined using organosolv lignin; this type of lignin is sulfur free, contains only trace amounts of carbohydrates, and is thought to retain a similar core

polymeric structure as that of milled wood lignin.[28] The data for these experiments is shown in Table 2. For all compounds, it was clear that lignin solubility increased with temperature. At 25 ºC, the mixtures were quite viscous, making mass transfer difficult, but at 90 ºC the mixtures were significantly less viscous. The order of lignin solubility is: $[C_2mim][Lys] > [C_2mim][OAc] > [Ch][Lys] > [Ch][OAc]$, which was inconsistent with the order of biomass delignification ($[C_2mim][Lys] \geq [Ch][Lys] > [Ch][OAc] \approx [C_2mim][OAc]$). ILs with imidazolium cations displayed higher organosolv lignin solubility as compared to ILs with ammonium cations. When holding the cation constant, ILs with $[Lys]^-$ dissolved more lignin than those with $[OAc]^-$. The majority of studies that address lignin solubility are limited to ILs with imidazolium based cations,[29] and π-π stacking interactions between imidazolium cations and phenyl groups found in lignin have been described.[11, 30] The anion is believed to catalyze or attack the β-O-4 linkages, thereby reducing the molecular weight of lignin.[31] In this 2 × 2 IL system, corroborated with our computational results, both electrostatics and π-π stacking interactions seemed to be the dominant non-covalent interactions contributing to the dissolution of organosolv lignin. It is interesting that lignin removal from switchgrass is improved 4.2-fold at 90 ºC and 1.7-fold at 140 ºC by using [Ch][Lys] as compared to $[C_2mim][OAc]$ (Table 1). The fact that $[C_2mim][Lys]$ and [Ch][Lys] are the best ILs in terms of lignin removal highlights the critical role of the anion. Since covalent linkages between lignin and hemicellulose in switchgrass often contain esters and hemiacetals, (i.e. ferulate/coumarate glycosides and 4-OMe glucuranoxylan), it is possible that either amide bonds or hemiaminals are being formed from the primary amine of $[Lys]^-$ *via* Kochetkov-type reactions (Figure S3). Either of these reactions could also account for the large amount of xylan removal by the $[Lys]^-$ containing ILs as compared to the $[OAc]^-$ ILs. This disparity is most apparent at 90 ºC (Table 1), and both amide formation and Kochetkov-type reactions are known to occur under mild conditions.[32]

3.2 Enzymatic hydrolysis after pretreatment

To compare enzyme kinetics and cellulose digestibility, enzymatic hydrolysis of untreated and pretreated switchgrass was carried out using commercial enzyme cocktails, Novozymes

Cellic® CTec2 and HTec2. For each sample, enzyme loadings were normalized to glucan content as determined by acidolysis. Pretreated switchgrass was used without drying, and solid loading (as 10% dry weight in the hydrolysis slurry) was calculated based on moisture content determined for each sample. Glucan and xylan yields after 72 h are plotted in Figure 2. After IL pretreatment, significantly faster saccharification rates and higher sugar yields were achieved. At higher temperatures, all glucose yields were above 90% with final glucose concentrations reaching 65 g/L. Most glucan to glucose conversion was complete after 48 h of enzymatic hydrolysis. Pretreatment at lower temperature resulted in glucan digestibility in the following the order: $[C_2mim][Lys] > [Ch][Lys] \approx [C_2mim][OAc] > [Ch][OAc]$. Thus, both cations and anions play critical roles in the biomass pretreatment mechanism. With regard to glucose conversion, ILs with $[Lys]^-$ were more efficient than ILs with $[OAc]^-$. When the anion was held constant, ILs containing $[C_2mim]^+$ were superior to those with $[Ch]^+$. Xylose conversion was similar to glucose conversion, with over 90% theoretical yield attained after pretreatment at 140 ºC for 1 h. With pretreatment conditions at 90 ºC xylan digestibility follows the order: $[Ch][Lys] \geq [C_2mim][Lys] > [Ch][OAc] \geq [C_2mim][OAc]$. Although the $[Lys]^-$ was still superior than $[OAc]^-$ for xylose conversion, the $[Ch]^+$ is slightly more effective than $[C_2mim]^+$ (Figure 3a).

In the literature, enzyme hydrolysis yields are often reported without considering glucan loss during pretreatment. Glucose and other sugars can be recovered using liquid-liquid extraction processes and must be accounted for in order to accurately report overall sugar yields for the entire conversion process[33] As shown in Table 3, the overall hydrolysis yields are calculated using the glucan recovery during the pretreatment (Eq. 3). Higher temperature pretreatment results in higher overall glucose yield, except with $[C_2mim][Lys]$. At the lower temperature pretreatment condition, both $[C_2mim][Lys]$ and $[Ch][Lys]$ outperformed $[C_2mim][OAc]$ with regards to glucose yield. $[C_2mim][Lys]$ gives lower xylose yield due to the poor xylan recovery after pretreatment. Lower enzyme loading (5 mg protein/g glucan) was also applied on the pretreated substrates generated, and the results are shown in Figure 4. Although the trends are similar to the results at the higher loading (20 mg protein/ g glucan; Figure 2-3, Table 3), the

glucose yields decreased significantly indicating the active sites of the pretreated substrate was not saturated with enzyme.

3.3 Kamlet-Taft parameters of the four ILs

All three K-T parameters are determined spectrophotometrically using a series of dyes as described in the experimental section. β values are considered to be a good predictor of IL pretreatment efficacy because the anion attracts hydroxyl protons of cellulose, disrupting the crystal lattice.[18] Pretreatment in ILs with $[OAc]^-$ (β >1.0) results in significant lignin removal (>32%), reduced cellulose crystallinity, and > 65% glucose yields after 12 h of cellulase hydrolysis.[18] ILs with lower β values (β ≤ 0.6) removes only 19% lignin, do not decrease cellulose crystallinity, nor improve sugar yields as compared to untreated biomass.[18] K-T parameters from the four ILs used in this study are given in Table 4, and Figure 5 shows temperature dependence of their β and π* values. Since [Ch][OAc] has a high melting point (ca. 85 ºC), its parameters could not be determined at temperatures lower than 85 ºC. We also found that K–T parameters for [Ch][OAc] could not be determined at temperatures ≥ 100 ºC due to disappearance of the absorption peak. As expected, ILs with the same anion showed similar β values, and ILs containing $[Lys]^-$ displayed higher β values and lower π* values as compared to ILs containing $[OAc]^-$. In all ILs tested, β values increased with increasing temperature. In a plot of K–T parameters vs. 1000/temperature (Figure 5), the slope of $[OAc]^-$ containing ILs is steeper, indicating that β values from these ILs increase faster with increasing temperatures. At 140 ºC, the β value (obtained by extrapolation) of $[C_2mim][OAc]$ is closer to the two $[Lys]^-$ ILs. This is consistent with the hydrolysis data for the four ILs where glucose yields are similar after pretreatment at higher temperatures. Figure 7b shows the correlation between glucose yield and β values; a general trend clearly shows that biomass pretreated with ILs with higher β values yields greater glucose after enzymatic hydrolysis.

3.4 Powder X-ray diffraction (PXRD)

PXRD was used to determine the proportions of crystalline and non-crystalline (i.e. amorphous cellulose, hemicelluloses and lignin) components found in the switchgrass sample,

and to monitor the structural changes in these polymers that occur during IL pretreatment. Commercial Avicel was used as a cellulose standard to validate the results. The XRD patterns are plotted in Figure 6 with CrI values noted on each spectrum. After pretreatment at 90 ºC for 5 h, all pretreated switchgrass showed diffraction patterns characteristic of the cellulose I polymorph. All the samples are semi-amorphous with different degrees of crystallinity (Figure 6a). Switchgrass pretreated with [C_2mim][OAc] has the lowest CrI value (22%) due to the partial swelling of the cellulose matrix. Switchgrass pretreated with the other three ILs has increased CrI values compared to raw switchgrass ([Ch][OAc]: 39% < [Ch][Lys]: 45% < [C_2mim][Lys]: 47%). During the pretreatment process, there are two competing factors that determine the crystallinity of the recovered solids: 1) decrystallization by swelling and dissolution of the crystalline cellulose portion, and 2) increase in CrI by reducing amorphous cellulose, lignin and hemicelluloses. The increased CrI values indicate that amorphous components removal is the dominant mechanism governing pretreatment with [Ch][OAc], [Ch][Lys] and [C_2mim][Lys]. These data are consistent with the compositional analysis (Table 1) showing the highest lignin and hemicelluloses removal after pretreatment with [C_2mim][Lys].

After pretreatment at 140 ºC for 1 h, only [C_2mim][OAc] pretreated switchgrass displayed a cellulose II crystal structure, different from the starting material (cellulose I). Pretreatment with [C_2mim][OAc] at 140 ºC caused disappearance of the broad peak at ca. 15-16º, representing a combination of the 101 and $10\bar{1}$ planes of cellulose I. The material is highly amorphous with a broad peak around 21°, which is assigned to the 002 cellulose II lattice plane.[34] This indicates that [C_2mim][OAc] has disrupted the crystal structure of cellulose during the higher temperature pretreatment. [Ch][OAc] pretreated switchgrass showed a decreased CrI value indicating some swelling/solvation of cellulose crystalline matrix. Pretreated switchgrass with [C_2mim][Lys] and [Ch][Lys] retains the highly crystalline cellulose I structure suggesting that the removal of amorphous components still dominates the process even at higher temperature pretreatment conditions.

To further understand cellulose structural changes during pretreatment, Avicel was pretreated using the same conditions as those used for switchgrass (Figure 6 left). After pretreating Avicel in [C_2mim][OAc] or [C_2mim][Lys] at 90 and 140 ºC the products display X-ray diffraction patterns indicative of cellulose II with characteristic diffraction peaks at ~ 12.1°, 20.0°, and 21.7°.[35] CrI of pretreated Avicel decreased dramatically after pretreatment with [C_2mim][OAc] or [C_2mim][Lys] (Avicel: 75%, Treated Avicel with [C_2mim][OAc]: 24% or 25%; Treated Avicel with [C_2mim][Lys]: 35% or 31%). These results indicate that both [C_2mim][OAc] and [C_2mim][Lys] solubilize cellulose. Conversely, the crystalline structure of [Ch][Lys] and [Ch][OAc] pretreated Avicel remained the same as untreated Avicel (i.e. cellulose I) with slightly decreased CrI (Avicel: 75%, Treated Avicel with [Ch][Lys]: 66%, 67%; Treated Avicel with [Ch][OAc]: 51%, 42%). Interference by amorphous polymers such as lignin and hemicellulose could have shifted the (002) peak of switchgrass slightly to the left as compared to that of Avicel. After pretreatment with [Ch][Lys] the (002) peak re-aligned with the (002) peak in Avicel, giving additional evidence to support significant removal of amorphous cell wall components by this IL.

As shown in Figure 7, the high sugar yields are generally obtained from high delignification due to pretreatment with ILs with large β values (Figure 7a,b). Contrary to literature reports,[18] we found no correlation of β values with glucan digestibility and substrate crystallinity (Figure 7b,c), indicating that it is still not clearly understood how anions and cations interact with cellulose or lignin. Therefore, we performed a theoretical study on the interaction of both cations and anions with lignin model compounds to further probe the mechanism of the high lignin removal by lysinate-based ILs.

3.5 Theoretical aspects of IL-Lignin interactions

Experimental and theoretical studies have been used to probe interactions between cellulose and ILs.[12, 36] Most recently, we reported conformational changes of the cellulose Iβ structure when dissolved in [C_2mim][OAc].[37] Molecular dynamics (MD) simulations showed strong

interactions between $[OAc]^-$ anions and the hydroxyl groups of cellulose. Detailed quantum mechanical (QM) studies combined with experimental data were used to characterize the interaction of the cellulose subunit (1,4)-dimethoxy-β-D-glucose with $[C_2mim][OAc]$.[38] Wang and coworkers have investigated the interaction of lignol with 1-allyl-3-methylimidazolium chloride ([Amim][Cl]).[39] It was observed that strong hydrogen bonding interactions between [Amim][Cl] and lignin hydroxyl groups were responsible for disrupting the internal network within the lignin, leading to its dissolution.[39, 40] Using dispersion-corrected density functional theory (DFT), Janesko reported significant π-stacking and hydrogen bonding interactions exist between an imidazolium cation / monolignol complex.[41] The degree of lignin removal is presumably proportional to the strength of the interactions between the cation and anion with lignin relative to the strength of interactions among cations and anions with each other, and/or with antisolvent. To evaluate this notion, we performed detailed quantum mechanical (QM) calculations to partition these various energy contributions for the four ILs studied to generate a more robust understanding of how they interact with a model biaryl compound.

Interaction between ions or ion pairs and lignin model compound: Dissecting the influence of the anion and cation on lignin dissolution remains a challenge, one that requires a comparative study of ILs interacting with lignin. We evaluated these effects by performing QM calculations of the four ILs interacting with a model dilignol compound of two arene rings connected by a β-O-4 linker (Figure 8). $[C_2mim]^+$ and $[Ch]^+$ were attracted to the electronegative regions of the dilignol model compound (Figure S5). A similar trend, albeit at a different locality on the dilignol, was observed when $[OAc]^-$ and $[Lys]^-$ preferred to interact with electropositive regions surrounding the dilignol. From the calculated IEs, it was also found that anions interact with dilignol more strongly than cations, and the IE of $[OAc]^-$ is higher than that of $[Lys]^-$. In the case of cation-dilignol interactions, our calculations show a higher IE for $[Ch]^+$ than for $[C_2mim]^+$, which is most probably due to larger electrostatics and higher hydrogen bonding energies. A previous theoretical study of model monolignol with $[C_2mim]^+$ indicated that π-stacking and hydrogen bonding interactions dominated the interaction [41]. However, our calculations demonstrate that $[C_2mim]^+$ interactions with a more

biologically relevant dilignol, containing hydroxyl groups in the linkage, are governed by strong electrostatic and hydrogen bonding interactions.[39]

We further quantified these interactions by evaluating the IEs of the ILs with dilignol. The molecular structures of all four IL ion pair-dilignol complexes as obtained from M06-2X/6-31+G (d, p) calculations along with their calculated BSSE corrected IEs at higher levels are shown in Figure 8. It was found that the IE strength followed the order [Ch][OAc] > [C_2mim][OAc] > [Ch][Lys] > [C_2mim][Lys]. As expected, the trend is consistent with the calculated IEs for individual ions interacting with dilignol. Surprisingly, experimental results for lignin solubility were found to be opposite of those determined computationally. In general, it appears there are tradeoffs between the degree to which the cation and anion interact with each other and the strength of interaction between the anion and cation with lignin. In the case of the four ILs studies here (IEs given in Supporting Information Figure S6), the top performing IL, [C_2mim][Lys], has the weakest self-interactions, freeing both $[Lys]^-$ and $[C_2mim]^+$ to solvate lignin, albeit less strongly than $[OAc]^-$ and $[Ch]^+$. The IL least able to solubilize lignin, [Ch][OAc], has the greatest self-interaction energy, suggesting it is too strongly coupled to effectively free its ions to interact with lignin.

Interaction energy in solvent phase: The dielectric environment may also influence bulk properties of IL solubility of lignin and changes upon addition of anti-solvent (water). The anti-solvent plays an important role in lignin removal since the lignin/IL solution is diluted significantly with water after pretreatment. In order to further probe the delignification trend observed between experiments and modeling results of ILs with dilignol, we investigated the effect of water solvation on IL-dilignol complexes mimicking the last experimental step in the pretreatment process. We employed an implicit solvation model (SMD is a solute density based model) at the M06-2X/6-311++G(d, p) level of theory. Table 6 summarizes the calculated BSSE corrected IEs in the solvent phase (water) using geometries optimized from gas phase models of the four IL-dilignol complexes. As shown in Table 6, the IEs of the four IL-dilignol complexes follow the order [Ch][Lys] > [C_2mim][Lys] > [Ch][OAc] > [C_2mim][OAc]. Earlier studies have shown that hydrogen bonding interactions between lignin and ILs

were weakened or even destroyed by the addition of water.[39] Accordingly, the IEs calculated from our solvent phase calculations are also much lower for ILs and dilignol complexes. Interestingly, $[Lys]^-$ containing ILs have marginally more binding affinity with dilignol than $[OAc]^-$ based ILs in the aqueous phase, and this affinity reflects that these ILs enable more lignin removal. These results are in agreement with the experimental results obtained.

Conclusions

ILs combining benchmark and biogenic cations and anions were evaluated as pretreatment solvents using two different pretreatment conditions (90 ^oC/5 h and 140 ^oC/1 h). ILs containing the lysinate anion outperformed acetate-containing ILs, in terms of glucose yield and delignification under both conditions. Specifically, $[C_2mim][Lys]$ removed up to 87% of the lignin found in switchgrass, showing great potential for industrial processes requiring biomass delignification and/or lignin conversion. Kamlet-Taft parameters showed significantly higher β values for $[Lys]^-$ containing ILs as compared to $[OAc]^-$ containing ILs. Though previous reports show that high β values are associated with both biomass dissolution and decreased CrI of pretreated biomass, our system showed that higher β values are only associated with higher lignin removal and greater sugar yields.

Non-covalent interactions between individual ions/ion pairs and our model dilignol compound suggested that the antisolvent significantly influenced the interaction energies governing lignin removal. The preferential interaction affinity of $[Lys]^-$ in solvent phase explains the higher delignification by these ILs compared to $[OAc]^-$ based ILs. To understand and optimize performance mechanisms of task specific ILs, a process model should consider factors ranging from solvent polarity properties, polymer solubility (i.e. lignin/cellulose/hemicellulose), as well as pretreatment severities. We have established a linkage between IL pretreatment efficiency, the experimentally determined Kamlet-Taft parameters, and computationally predicted interaction energies. This predictive capability and the insights it provides will assist in developing subsequent novel combinations of anions and cations for biomass pretreatment.

Acknowledgments

This work conducted by the Joint BioEnergy Institute was supported by the Office of Science, Office of Biological and Environmental Research, of the U.S. Department of Energy under Contract No. DE-AC02-05CH11231. This research used resources of the National Energy Research Scientific Computing Center (NERSC) and the authors thank Francesca Verdier, Department Head, NERSC Services for the timely help. The authors also thank Dr. Dong Wu for providing the cell wall image in the graphical table of contents entry.

504 **Table 1.** Compositional analysis after IL pretreatment
505
506

Pretreatment			Composition of pretreated biomass (%)			Removal after pretreatment (%)		
ILs	**T/t**	**Solid recovery (%)**	**Glucan**	**Xylan**	**Lignin**	**Glucan**	**Xylan**	**Lignin**
-			37.5 ±1.5	21.9±2.0	18.9±1.3			
[C_2mim][OAc]	90/5	92.3±5.7	38.0±3.2	23.5±3.3	17.1±1.2	6.5±2.3	1.0±2.5	16.5±0.9
[C_2mim][Lys]	90/5	58.2±0.2	65.2±1.3	18.9±0.6	6.4±0.4	-1.2±2.8	49.8±1.4	80.3±1.4
[Ch][Lys]	90/5	70.7±4.9	49.2±0.9	21.7±0.2	8.2±0.6	7.2±2.4	29.9±4.1	69.3±0.01
[Ch][OAc]	90/5	87.2±4.4	40.2±2.4	24.7±2.8	18.0±1.3	6.5±2.4	1.7±0.7	17.0±1.8
[C_2mim][OAc]	140/1	70.5±0.3	50.0±1.0	21.2±1.1	13.7±0.2	6.0±1.3	31.8±3.6	48.9±0.8
[C_2mim][Lys]	140/1	50.8±0.3	63.2±0.1	17.2±1.0	5.0±0.9	14.4±0.6	60.1±2.5	86.6±3.3
[Ch][Lys]	140/1	56.6±0.7	65.6±3.6	23.9±0.1	5.0±0.1	6.0±2.3	38.2±0.5	85.1±0.1
[Ch][OAc]	140/1	66.7±0.3	49.8±1.8	20.8±2.8	14.1±1.0	11.4±2.8	36.7±1.2	50.2±4.1

507

Table 2. Lignin solubility in different ILs at 25 °C and 90 °C

ILs	25 °C		90 °C	
	%*	g/L	%*	g/L
[C_2mim][OAc]	5	55	15	165
[C_2mim][Lys]	15	165	22	242
[Ch][Lys]	< 3	< 33	10	110
[Ch][OAc]	N/A‡	N/A‡	5	55

*gram of lignin / gram of IL × 100%

‡: The solubility of lignin could not be determined since [Ch][OAc] is solid at RT.

Table 3. Overall glucose yield after enzymatic saccharification

ILs	T/t	Glucan Recovery (%)			Xylan Recovery (%)		
		Glucan rec.[a]	Glc yield[b]	Overall glc yield[c]	Xylan rec.[a]	Xyl yield[b]	Overall xyl yield[c]
[C_2mim][OAc]	90/5	93.5	77.5	72.5	99.0	56.2	55.6
	140/1	94.0	95.8	90.1	68.2	93.3	63.6
[C_2mim][Lys]	90/5	100.0	91.3	91.3	50.2	76.4	38.4
	140/1	85.6	96.4	82.5	39.9	95.9	38.3
[Ch][Lys]	90/5	92.8	83.9	77.9	70.1	95.0	66.6
	140/1	99.0	96.5	95.5	61.8	95.7	59.1
[Ch][OAc]	90/5	93.5	60.0	56.1	98.3	58.2	57.2
	140/1	88.6	93.5	82.8	63.3	95.0	60.1

a. Glucan recovery/xylan recovery is percentage of recovered glucan/xylan after pretreatment (calculate based on glucan/xylan present in untreated switchgrass, Eq 3);
b. Glucose yield/xylose yield is glucose/xylose yield after enzymatic saccharification (calculate based on glucan/xylan present in pretreated switchgrass);
c. Overall glucose/xylose yield represents the overall sugar yield considering the whole process (both pretreatment and enzymatic saccharificaton)

Table 4. Kamlet-Taft parameters of the ILs

ILs	π		α		β	
	30 °C	90 °C	30 °C	90 °C	30 °C	90 °C
[C_2mim][OAc]	1.04	0.91	0.47	0.51	1.14	1.23
[C_2mim][Lys]	0.64	0.60	N/D*	N/D	1.28	1.29
[Ch][Lys]	0.67	0.64	N/D*	N/D*	1.30	1.31
[Ch][OAc]	N/A‡	0.76	N/A‡	0.68	N/A	1.22

*: α value of [C_2mim][Lys] and [Ch][Lys] could not be determined since no peak was observed with Reichardt's dye

‡: The parameters of [Ch][OAc] at 30 °C could not be determined since the melting point of [Ch][OAc] is 85 °C.

Table 5. Calculated Interaction Energies (IEs in kcal/mol) of dilignol - ILs complexes

ILs	IE in implicit water with dilignol
[C_2mim][OAc]	9.32
[Ch][OAc]	12.18
[C_2mim][Lys]	13.52
[Ch][Lys]	14.58

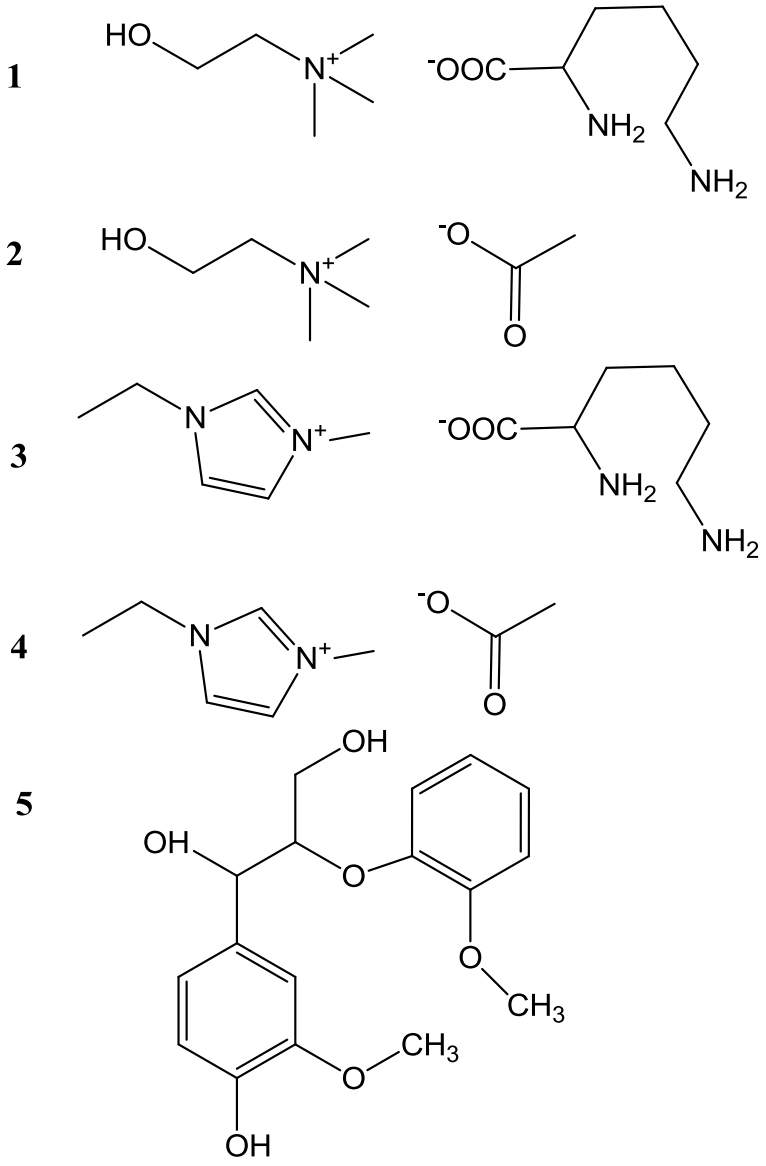

Figure 1. Ionic liquids used in this study and the dilignol used for quantum chemical calculations. [Ch][Lys] (**1**), [Ch][OAc] (**2**), [C_2mim][Lys] (**3**), [C_2mim][OAc] (**4**), and dilignol model compound (**5**).

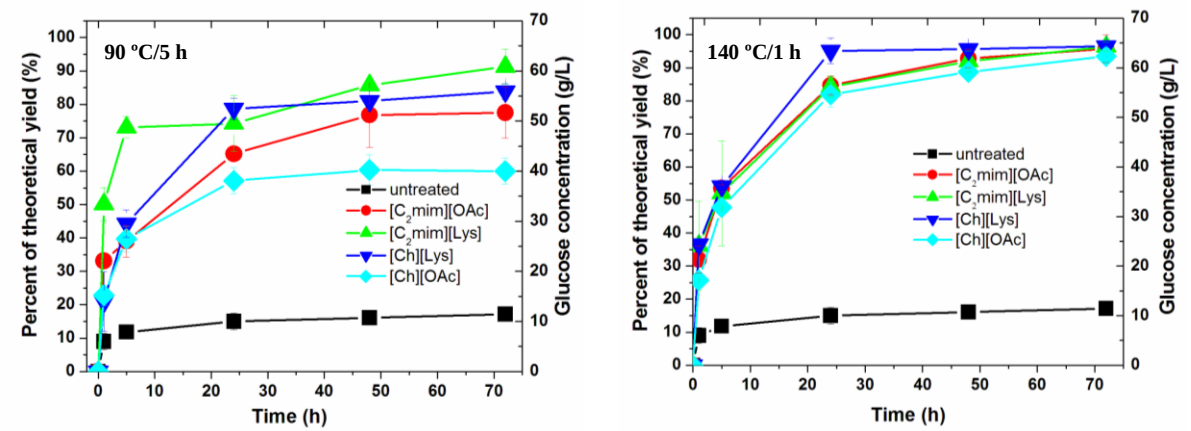

Figure 2. Glucan digestibility of the pretreated switchgrass with two different pretreatment conditions (enzyme loading: 20 mg protein /g glucan). Left: 90 ºC/5 h, right: 140 ºC/1 h.

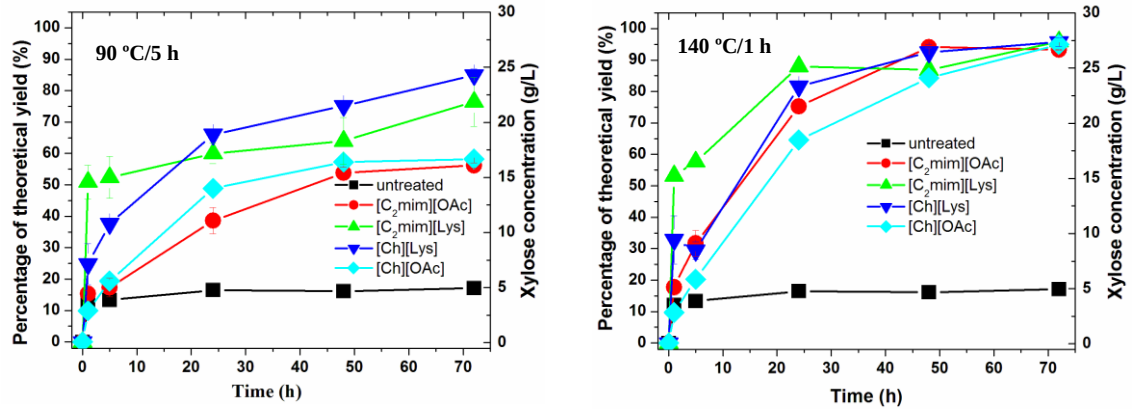

Figure 3. Xylan digestibility of the pretreated switchgrass with different pretreatment conditions (enzyme loading: 20 mg protein /g glucan). Left: 90 ºC/5 h, right: 140 ºC/1 h.

.

560

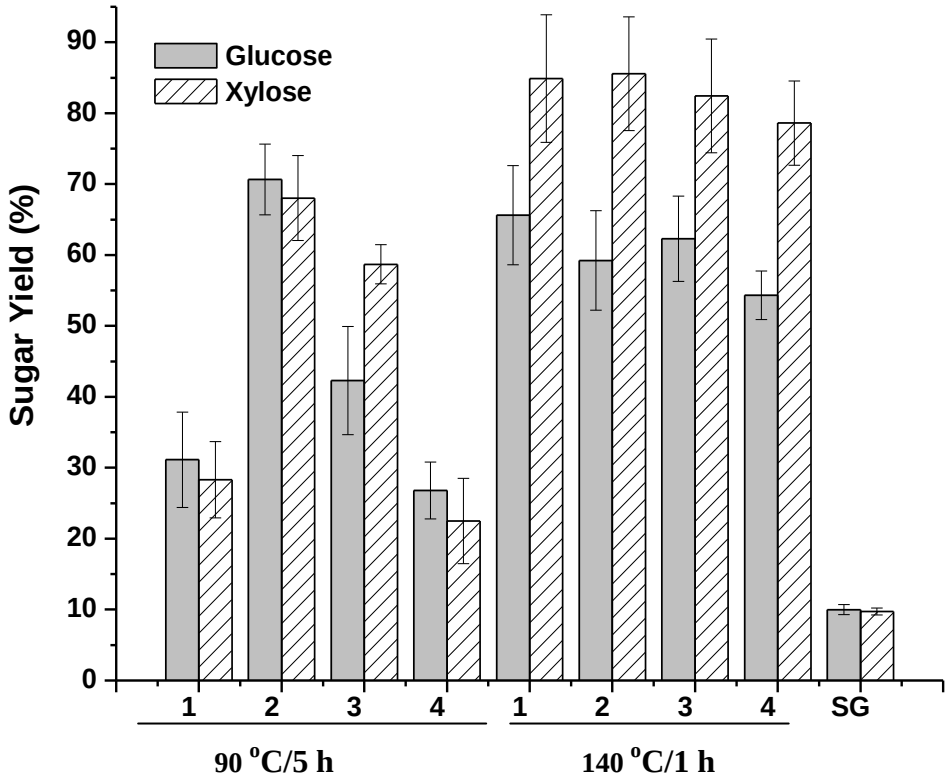

561

562 **Figure 4.** Glucose and xylose yields of the pretreated biomass after 72 h enzymatic
563 saccharification (enzyme loading: 5 mg protein /g glucan). The numbers on the x axis represent
564 different ILs: 1, [C_2mim][OAc]; 2, [C_2mim][Lys]; 3, [Ch][Lys]; 4, [Ch][OAc], SG:
565 switchgrass.

566

567

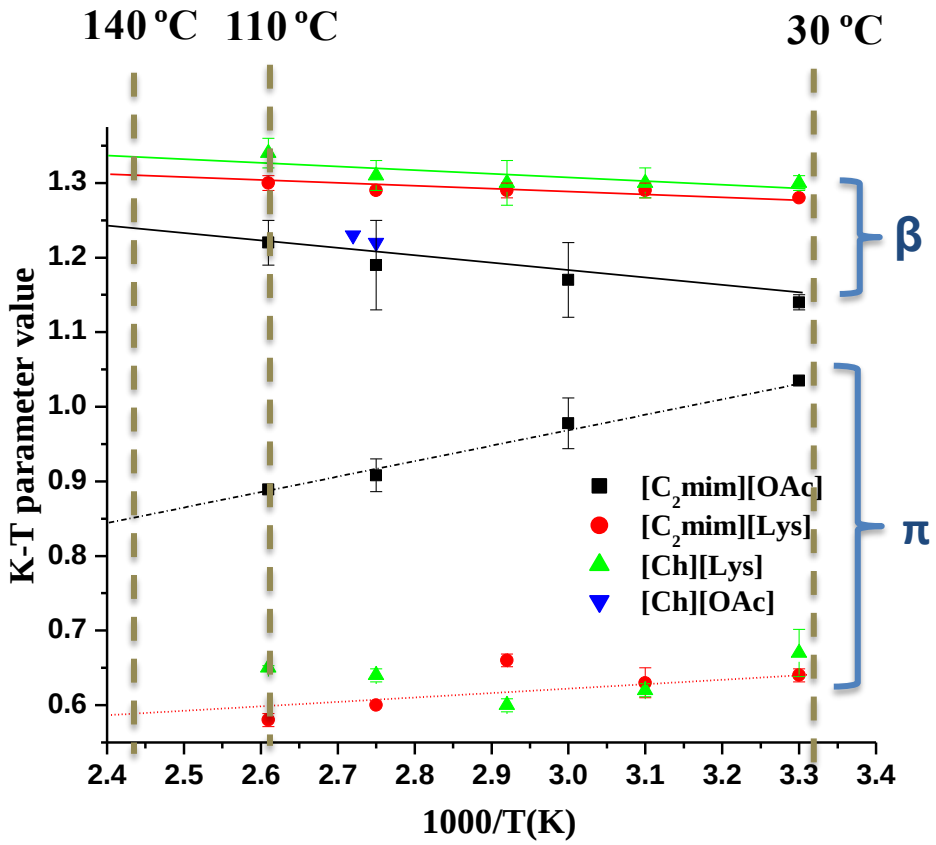

Figure 5. K-T parameter of the ILs at different temperatures

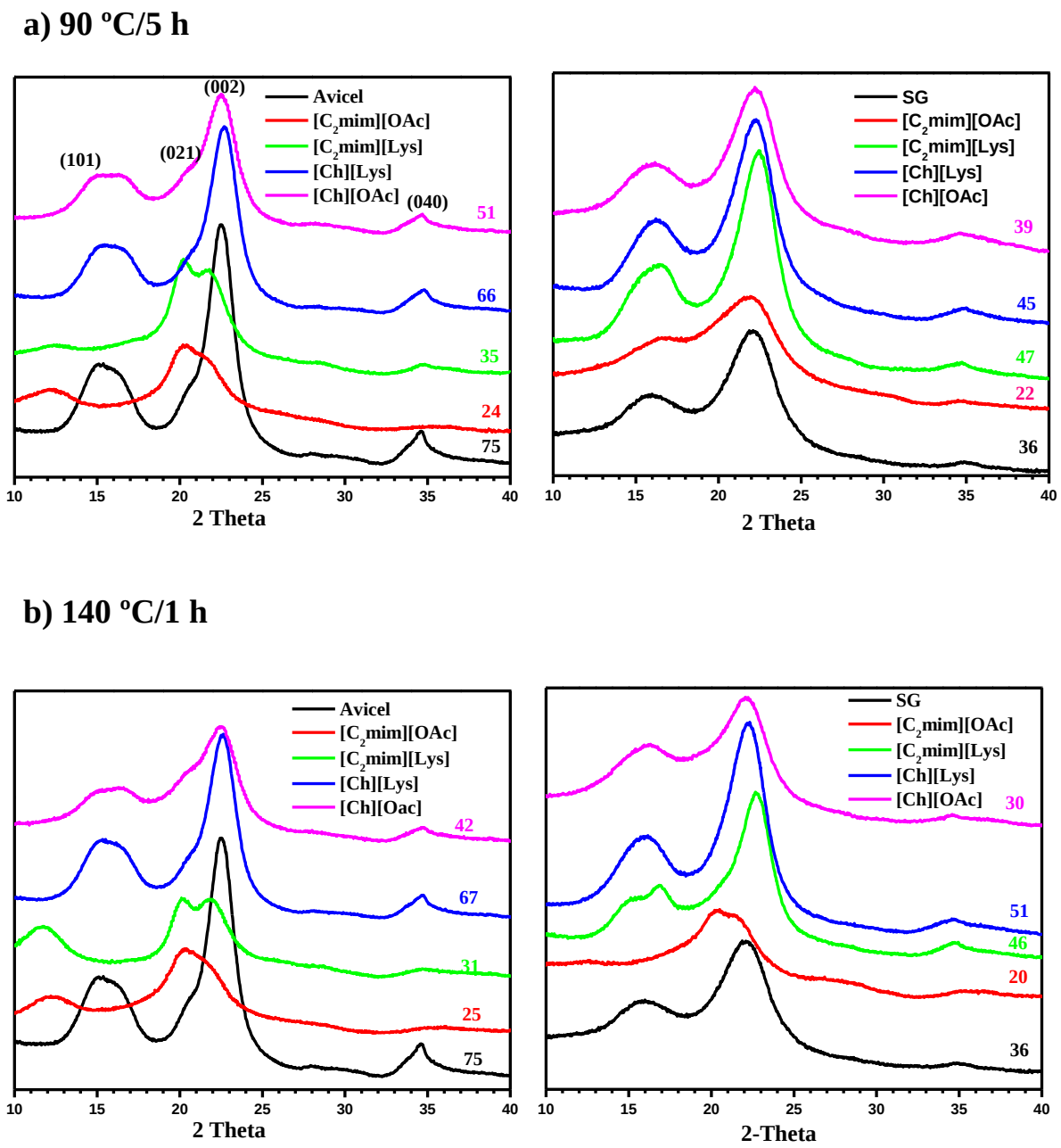

Figure 6. X-ray diffraction patterns and CrI (%) value (noted on the right side of each spectrum) of pretreated Avicel (left) and biomass (right) with different pretreatment conditions: a) 90 °C for 5 h; b) 140 °C for 1 h.

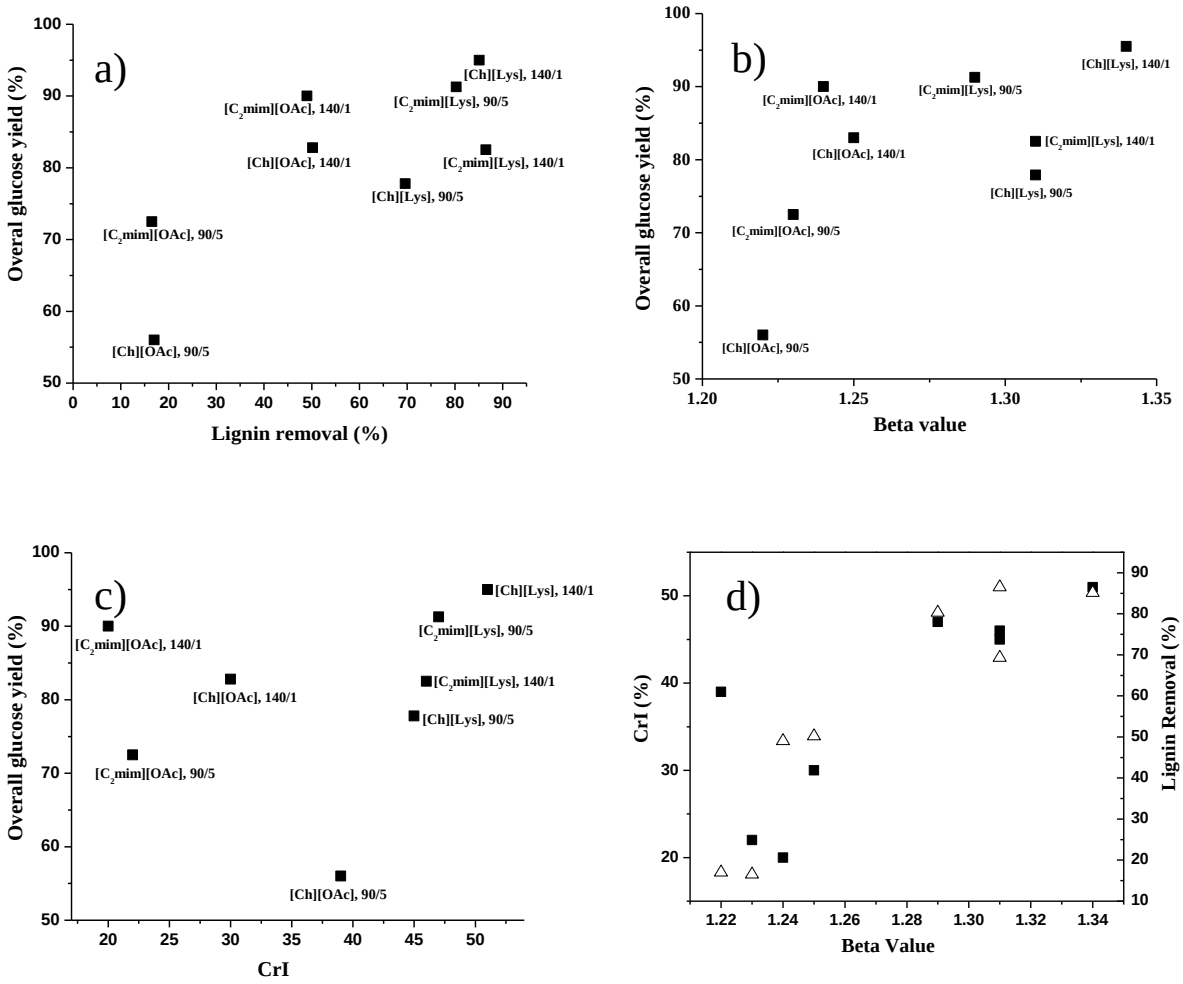

Figure 7. Correlation between the major factors during the process: overall glucose yield vs. lignin removal (a), overall glucose yield vs. β value (b), overall glucose yield vs. CrI (c), CrI vs. β value (d, square), and lignin removal vs. β value (d triangle).

586

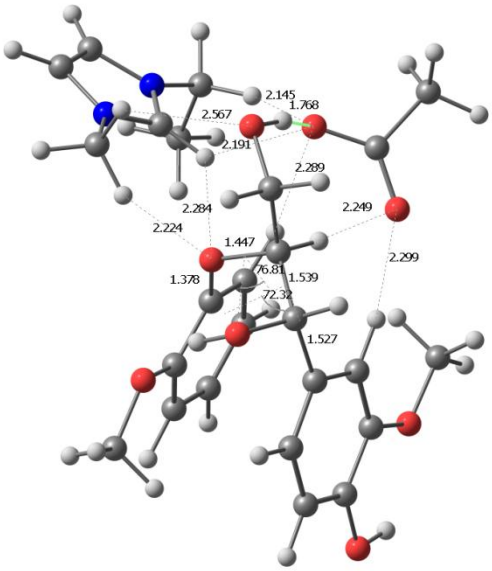

[C_2mim]$^+$[OAc]— dilignol
IE=134.28

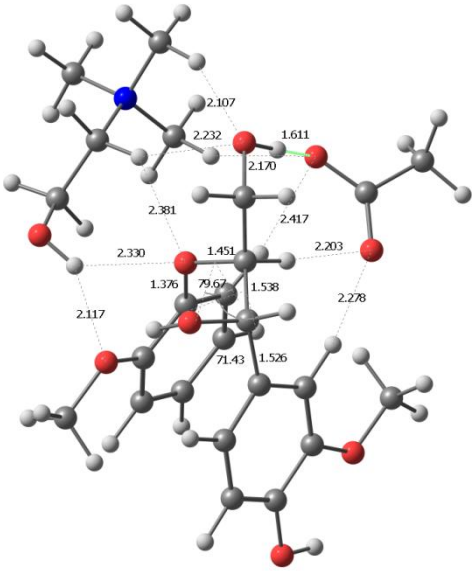

[Ch]$^+$[OAc] — dilignol
IE=139.73

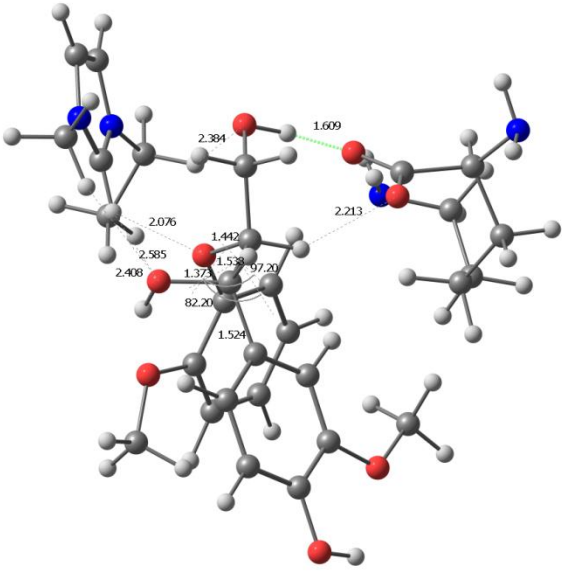

[C_2mim]$^+$[Lys] — dilignol
IE=123.25

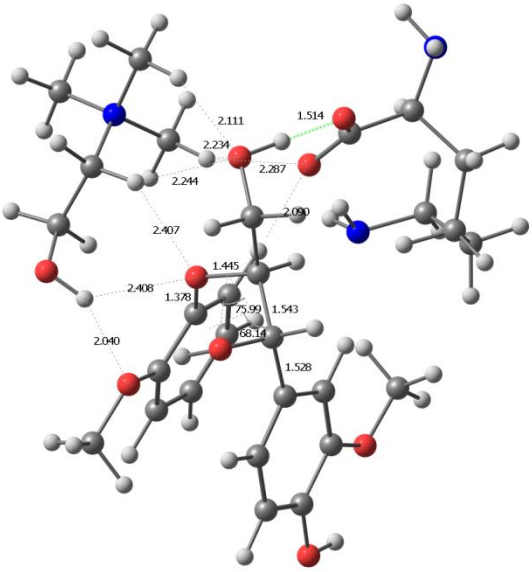

[Ch]$^+$[Lys] — dilignol
IE=132.72

587

588 **Figure 8.** Optimized geometries of dilignol with four IL complexes. Interaction energy (IE) is
589 reported in kcal/mol.

590

591

592

4. References

1. R. P. Swatloski, S. K. Spear, J. D. Holbrey and R. D. Rogers, *Journal of the American Chemical Society*, 2002, 124, 4974-4975.
2. A. P. Dadi, S. Varanasi and C. A. Schall, *Biotechnology and Bioengineering*, 2006, 95, 904-910.
3. S. H. Lee, T. V. Doherty, R. J. Linhardt and J. S. Dordick, *Biotechnology and Bioengineering*, 2009, 102, 1368-1376.
4. B. A. S. Seema Singh, Kenneth P. Vogel,, *Biotechnology and Bioengineering*, 2009, 9999, n/a.
5. N. Sun, M. Rahman, Y. Qin, M. Maxim, H. Rodríguez and R. Rogers, *Green Chem.*, 2009, 11, 646-655.
6. C. Li, G. Cheng, V. Balan, M. S. Kent, M. Ong, S. P. S. Chundawat, Y. B. Melnichenko, B. E. Dale, B. A. Simmons and S. Singh, *Bioresour Technol*, 2011, 102, 6928-6936.
7. C. Li, B. Knierim, C. Manisseri, R. Arora, H. V. Scheller, M. Auer, K. P. Vogel, B. A. Simmons and S. Singh, *Bioresour Technol*, 2010, 101, 4900-4906.
8. A. G. Cruz, C. Scullin, C. Mu, G. Cheng, V. Stavila, P. Varanasi, D. Xu, J. Mentel, Y.-D. Chuang and B. A. Simmons, *Biotechnology for Biofuels*, 2013, 6, 1-10.
9. A. M. Socha, S. P. Plummer, V. Stavila, B. A. Simmons and S. Singh, *Biotechnology for Biofuels*, 2013, 6, 61.
10. S. S. Y. Tan, D. R. MacFarlane, J. Upfal, L. A. Edye, W. O. S. Doherty, A. F. Patti, J. M. Pringle and J. L. Scott, *Green Chem.*, 2009, 11, 339-345.
11. M. Zavrel, D. Bross, M. Funke, J. Buchs and A. C. Spiess, *Biores. Technol.*, 2009, 100, 2580-2587.
12. R. C. Remsing, R. P. Swatloski, R. D. Rogers and G. Moyna, *Chem. Commun.*, 2006, 1271-1273.
13. M. J. Kamlet, J. L. Abboud and R. Taft, *Journal of the American Chemical Society*, 1977, 99, 6027-6038.
14. M. Ab Rani, A. Brant, L. Crowhurst, A. Dolan, M. Lui, N. Hassan, J. Hallett, P. Hunt, H. Niedermeyer and J. Perez-Arlandis, *Physical Chemistry Chemical Physics*, 2011, 13, 16831-16840.
15. A. Xu, J. Wang and H. Wang, *Green Chemistry*, 2010, 12, 268-275.
16. L. K. J. Hauru, M. Hummel, A. W. T. King, I. A. Kilpeläinen and H. Sixta, *Biomacromolecules*, 2012, 13, 2896-2905.
17. A. Brandt, J. P. Hallett, D. J. Leak, R. J. Murphy and T. Welton, *Green Chem*, 2010, 12, 672-679.
18. T. V. Doherty, M. Mora-Pale, S. E. Foley, R. J. Linhardt and J. S. Dordick, *Green Chem.*, 2010, 12, 1967-1975.
19. X. D. Hou, T. J. Smith, N. Li and M. H. Zong, *Biotechnol. Bioeng.*, 2012, 109, 2484-2493.
20. A. Brandt, M. J. Ray, T. Q. To, D. J. Leak, R. J. Murphy and T. Welton, *Green Chem.*, 2011, 13, 2489-2499.
21. Q. P. Liu, X. D. Hou, N. Li and Z. M.H., *Green Chem.*, 2012, 14, 304-307.
22. K. Fukumoto, M. Yoshizawa and H. Ohno, *JACS*, 2005, 127, 2398-2399.
23. A. Sluiter, *National Renewable Energy Laboratory (NREL) Analytical Procedures*, 2004.
24. S. F. Boys and F. Bernardi, *Molecular Physics: An International Journal at the Interface Between Chemistry and Physics*, 1970, 19, 553 - 566.
25. M. J. T. Frisch, G. W.; Schlegel, H. B.; Scuseria, G. E.; Robb, M. A.; Cheeseman, J. R.; Montgomery, J. A., Jr.; Vreven, T.; Kudin, K.; Burant, J. C.;Gaussian 09, revision A.01; Gaussian, Inc: Wallingford, CT, 2009.
26. R. Arora, C. Manisseri, C. Li, M. D. Ong, H. V. Scheller, K. Vogel, B. A. Simmons and S. Singh,

***Bioenerg. Res.*, 2010, 3, 134-145.**

27. **W. Li, N. Sun and R. D. Rogers, *Green Chemistry*, 2011, 13, 2038-2047.**
28. **R. El Hage, N. Brosse, L. Chrusciel, C. Sanchez, P. Sannigrahi and A. Ragauskas, *Polymer Degradation and Stability*, 2009, 94, 1632-1638.**
29. **Y. Pu, N. Jiang and A. J. Ragauskas, *Journal of Wood Chemistry and Technology*, 2007, 27, 23-33.**
30. **I. Kilpeläinen, H. Xie, A. King, M. Granstrom, S. Heikkinen and D. Argyropoulos, *J. Agric. Food Chem.*, 2007, 55, 9142-9148.**
31. **A. George, K. Tran, T. Morgan, P. Benke, C. Berrueco, E. Lorente, B. Wu, J. Keasling, B. A. Simmons and B. Holmes, *Green Chem.*, 2011, 13, 3375-3385.**
32. **L. M. Likhosherstov, O. S. Novikova, V. A. Derevitskaja and N. K. Kochetkov, *Carbohydrate Research*, 1986, 146, C1-C5.**
33. **T. C. R. Brennan, S. Datta, H. W. Blanch, B. A. Simmons and B. M. Holmes, *Bioenerg. Res.*, 2010, 3, 123-133.**
34. **G. Cheng, P. Varanasi, R. Arora, V. Stavila, B. A. Simmons, M. S. Kent and S. Singh, *The Journal of Physical Chemistry B*, 2012.**
35. **P. Mansikkamäki, M. Lahtinen and K. Rissanen, *Cellulose*, 2005, 12, 233-242.**
36. **H. Liu, K. L. Sale, B. M. Holmes, B. A. Simmons and S. Singh, *The Journal of Physical Chemistry B*, 2010, 114, 4293-4301.**
37. **H. Liu, G. Cheng, M. Kent, V. Stavila, B. A. Simmons, K. L. Sale and S. Singh, *The Journal of Physical Chemistry B*, 2012, 116, 8131-8138.**
38. **Z.-D. Ding, Z. Chi, W.-X. Gu, S.-M. Gu, J.-H. Liu and H.-J. Wang, *Carbohydrate Polymers*, 2012, 89, 7-16.**
39. **W. Ji, Z. Ding, J. Liu, Q. Song, X. Xia, H. Gao, H. Wang and W. Gu, *Energy & Fuels*, 2012, 26, 6393-6403.**
40. **H. Lateef, S. Grimes, P. Kewcharoenwong and B. Feinberg, *Journal of Chemical Technology & Biotechnology*, 2009, 84, 1818-1827.**
41. **B. G. Janesko, *Phys. Chem. Chem. Phys.*, 2011, 13, 11393-11401.**

Table of Contents Entry

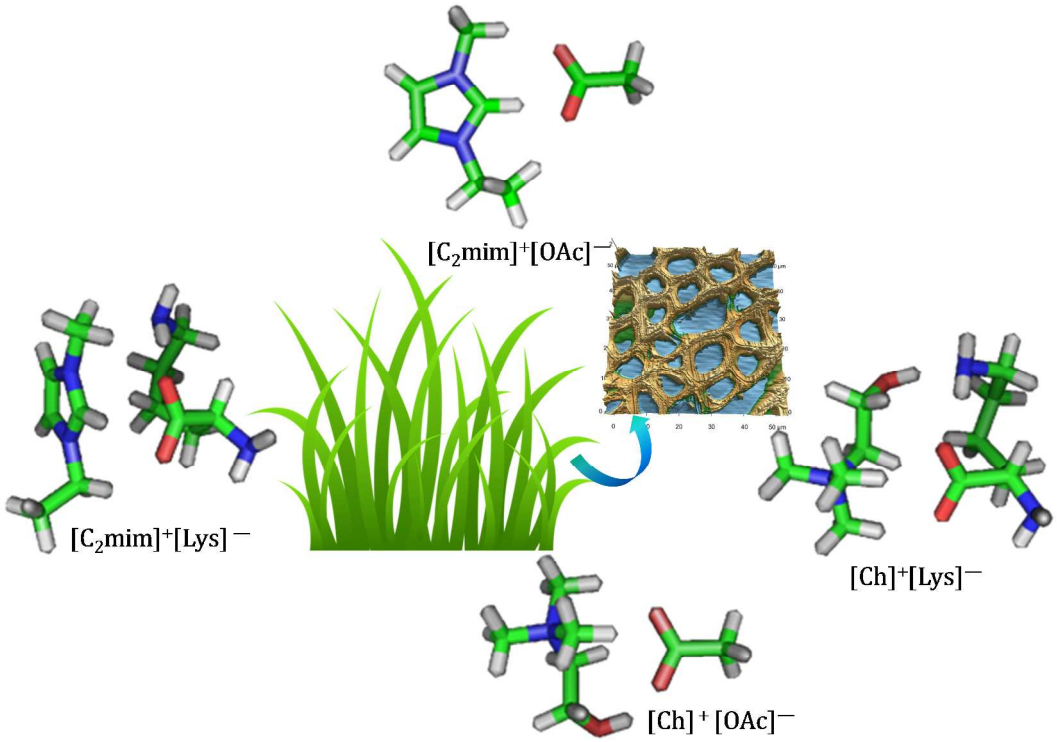

Text:

Understanding specific combinations of cations and anions of ionic liquids for biomass pretreatment.